MODELING CALCOFI OBSERVATIONS DURING EL NIÑO: FITTING PHYSICS AND BIOLOGY

ARTHUR J. MILLER, EMANUELE DI LORENZO,
DOUGLAS J. NEILSON, BRUCE D. CORNUELLE
Climate Research Division
Scripps Institution of Oceanography
University of California, San Diego
La Jolla, California 92093-0224
ajmiller@ucsd.edu

JOHN R. MOISAN
Observational Science Branch
Laboratory for Hydrospheric Processes
NASA GSFC/Wallops Flight Facility
Wallops Island, Virginia 23337-5099

ABSTRACT

Surveys of temperature, salinity, and velocity from CalCOFI, altimetric measurements of sea level, and drifter observations of temperature and velocity during the 1997–98 El Niño are now being fit with an eddy-resolving ocean model of the Southern California Bight region to obtain dynamically consistent estimates of eddy variability. Skill is evaluated by the model-data mismatch (rms error) during the fitting interval and eventually by forecasting independent data. Preliminary results of fitting July 1997 physical fields are discussed. The physical fields are used to drive a three-dimensional NPZD-type model to be fit to subsurface chlorophyll a (chl a), nitrate, and bulk zooplankton from CalCOFI surveys, and surface chl a from SeaWiFS. Preliminary results of testing the ecosystem model in one-dimensional and three-dimensional form are discussed.

INTRODUCTION

The California Cooperative Oceanic Fisheries Investigations (CalCOFI) program has sampled the oceanographic conditions of the Southern California Bight (SCB) for 50 years, providing an unprecedented time series of physical and biological data (e.g., Roemmich and McGowan 1995). However, our understanding of the physical processes controlling the large-scale and mesoscale variations in these properties is incomplete (e.g., Bograd et al., in press). In particular, the nonsynopticity and relatively coarse spatial sampling (70 km) of the hydrographic grid do not resolve the mesoscale eddy field (fig. 1a). Moreover, these physical variations exert a dominant influence on the evolution of the ecosystem (e.g., Hayward and Venrick 1998).

In recent years, additional data sets that partially sample the SCB have become available. Acoustic Doppler current profiler (ADCP) measurements now sample upper-ocean velocity between stations (fig. 1b) and give a more complete picture of the mesoscale (Chereskin and Trunnell 1996). Observations of sea level along TOPEX tracks (fig. 1c) give another partial view of the mesoscale, well-sampled along each track but coarsely sampled temporally and between tracks. Surface drifters occasionally pass through the region (fig. 1d). SeaWiFS provides estimates of upper-ocean chlorophyll a (chl a), usually giving nearly complete coverage after weeklong intervals (depending on cloud coverage).

In order to better interpret the dynamical balances of the physical and biological fields, we are attempting to use an ocean model to fuse together the various data types and develop a complete four-dimensional picture of the evolving flow field and its biology during a particular three-week cruise. This model-testing procedure is often called a fit. If the fit is successful, the model run can be used to assess the balances that control the evolving phenomena. If not, the model must be corrected or discarded. The final test of the model's quality is to determine if forecasting skill is present by running the model beyond the fitting time interval into the forecast time interval (independent data).

Assuming that unstable mesoscale eddies dominate the physical balances, one anticipates that model fitting and/or forecasting skill is achievable to at least the eddy turnaround time scale, which is roughly one to three months. If atmospheric forcing dominates the flow variability, such as in the surface mixed layer, then the fitting time scale is infinite (quantitatively limited only by the model's physics), and the forecasting time scale is the roughly weeklong time scale of atmospheric forecasting skill.

Unfortunately, these fitting and forecasting time scales are probably overestimated, because limited oceanographic data cannot yield unique solutions for the fits or unambiguous verifications for forecasts (e.g., Miller and Cornuelle 1999). However, the 1997–98 El Niño and the 1999–2000 La Niña time periods were sampled particularly well in the SCB, giving us a unique opportunity to test fitting and forecasting skill and to assess dynamic and ecosystem balances during these strongly anomalous warm and cold time periods.

The fundamental scientific issues to be ultimately addressed by this research are the relative importance of mesoscale instabilities, topographic control, remote oceanic forcing, and wind forcing in the evolution of eddies in the CalCOFI region; the relative predictive time scales of deep ocean versus surface processes versus shelf-slope processes; and the ecosystem balances.

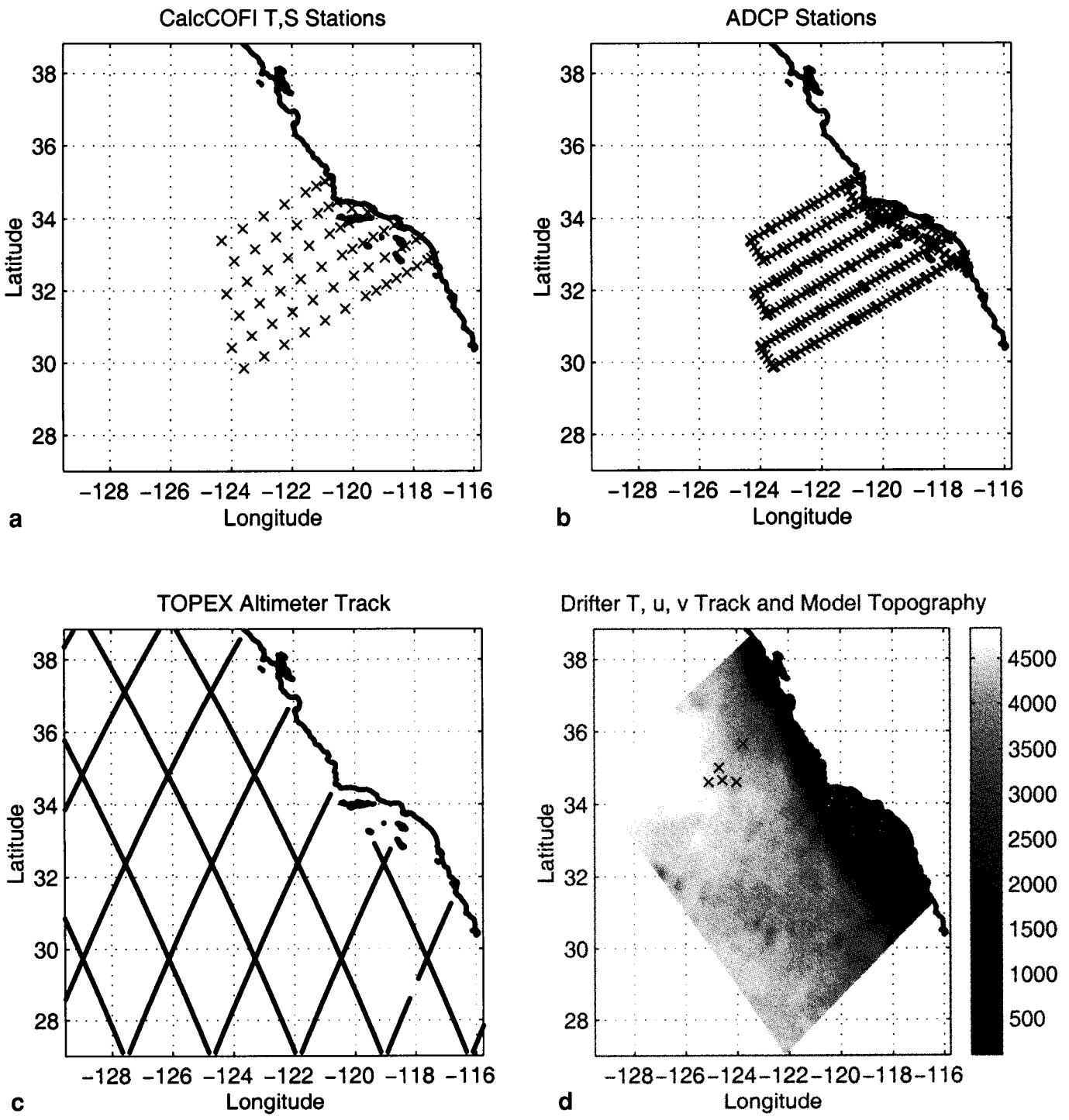

Figure 1. Distribution in space of the data types to be fit by the inverse method in the model domain for July 1997: *a*, CalCOFI hydrographic stations of temperature, salinity, nitrate, chl a, and bulk zooplankton; *b*, ADCP upper-ocean currents; *c*, sea level from TOPEX representing 9-day time differences; and *d*, drifter observations of 15 m velocity and SST, and bathymetry used in the model (m).

We report here our progress in fitting July 1997 hydrography, tuning one-dimensional ecosystem parameters based on historical CalCOFI data, and initializing three-dimensional ecosystem structure from data during February 1998.

DATA SOURCES

CalCOFI hydrographic data (*http://www-mlrg.ucsd.edu/calcofi.html*) from 1949 through 1999 were used for comparing against model results, and for creating first-guess initial and key background nudging conditions. The data

used herein for various purposes include temperature, salinity, density, oxygen, nitrate, chl a, and primary production rates.

Climatological profiles of the data were created by binning the offshore and coastal stations. Profiles of the coastal temperature, salinity, and nutrient climatologies show a marked seasonal 50 m doming of the isopleths with a maximum vertical shoaling in May, coincident with the seasonal maximum of California Current velocities. Offshore climatologies show little variability except in May and December, when the profiles show the presence of colder, nutrient-rich water. This variability has been attributed to sampling biases resulting from a change in the CalCOFI sampling schedule. In the last 15 years CalCOFI has not sampled in the months of May and December.

Further analysis of the CalCOFI data includes objective analysis (OA) to create maps of the data fields at model levels for first-guess initial conditions. These techniques are discussed in more detail in subsequent sections. Raw hydrographic observations are also used for quantifying fitting skill. ADCP velocity estimates are used as one-hour averages, which provide roughly five samples between CalCOFI hydrographic stations. TOPEX altimetric measurements of sea level are used as differences between nine-day repeat track times in order to remove geoid effects. Drifters provide daily surface velocity and temperature estimates. Atmospheric forcing is derived from COADS and NCEP/NCAR reanalysis fields.

Daily satellite-derived estimates of surface chl a were obtained from the NASA SeaWiFS data archive. We use the global gridded L3m data set, which has 9 km resolution. The satellite began collecting data in September 1997, so we presently have close to 2.5 years of images. The daily images are unfortunately incomplete in the CalCOFI region due to the frequent cloud cover offshore. Therefore, 5-day composite images have been created for use in developing initial conditions and quantitative model-data comparisons.

PHYSICAL AND ECOSYSTEM MODELS

We use an eddy-resolving primitive equation (PE) generalized sigma-coordinate ocean circulation model called the Regional Ocean Modeling System (ROMS), which is a descendant of SCRUM (Song and Haidvogel 1994). The 9 km model grid is curvilinear and extends about 1,200 km along the coast from northern Baja California to north of the San Francisco Bay area, with roughly 700 km offshore extent normal to the coast (fig. 1d). The northern, southern, and western boundaries are open, and are treated by using a modified version of the Orlanski radiation scheme or with nudging to specified time-dependent temperature and salinity values. We use ETOPO-5 for the bathymetry (fig. 1d) and the coastal masking along the eastern boundary. In the vertical, 20 layers reach from the free surface to the bottom of the ocean. The sigma layers are such that they have increased resolution in the surface and bottom boundary layers. In the shallow coastal region, the top layer can be as thin as 2 meters.

We initially tested the physical model with simple parameterizations of the external forcing and bathymetry, in order to verify its ability to capture the basic physics of the region. Integration with smooth climatological forcing (COADS data) showed that the statistics of the model are comparable with observations. Some of these features include a meandering current flowing from north to south, a poleward undercurrent on the continental slope, and a recirculation gyre in the SCB. In a qualitative analysis of the model results, we found the horizontal eddy length and time scales to be comparable with the observed eddies. A more quantitive measure of the model's skill is assessed by the fitting procedure described below.

The physical model drives a seven-component ecosystem model (either uncoupled or coupled via the light-absorption feedback) which includes nitrate, phytoplankton, ammonium, zooplankton, chl a, and two (large and small) detritus pools. The present model is similar in structure to the coupled ocean circulation ecosystem model developed and applied to the California coastal transition zone by Moisan et al. (1996). The simulated flow fields from the three-dimensional physical model are used to advect and diffuse the ecosystem's model constituents. The biological quantities are solved in the model as tracers with the addition of a nonlinear source/sink term that regulates the exchange between one biological variable and the other (e.g., Fasham et al. 1990).

The biological portion of the model, therefore, is a system of seven coupled partial differential equations that govern the spatial and temporal distribution of a nonconservative quantity, which is of the form

$$\frac{\partial B}{\partial t} = \nabla \cdot K \nabla B - (\vec{v} + \vec{v}_{\text{biology}}) \cdot \nabla B + S - r_{\text{nudge}}(B - B_{\text{clim}})$$

where ∇ is the 3D gradient, B is a nonconservative quantity (one of the seven components in the biological model), $\vec{v}$ is the vertical and horizontal velocity of the fluid, and $\vec{v}_{\text{biology}}$ is the vertical sinking rate of the biological components. The velocity, $\vec{v}$, and the kinematic eddy diffusivity, K, were obtained as described below. The source or sink term, S, for the biological component is defined by the sum of the individual forcing terms associated with the ecosystem model, and r_{nudge} is the

rate at which the biological component is nudged back to the climatological mean of the biological component, B_{clim}. In this study, the climatological fields will be used to relax only the deep-water values over a long time scale so that climate drift of the deep-water nutrient fields can be avoided.

INVERSE METHOD FITTING TECHNIQUE

Many techniques exist for combining data with models (e.g., reviews by Ghil and Malanotte-Rizzoli 1991; Bennett 1992; Wunsch 1996). Least-squares methods are widely used for fitting both steady and unsteady models to data, and can be implemented sequentially as the Kalman smoother, or globally by solving the Euler-Lagrange equations to find the minimum of an objective function (Le Dimet and Talagrand 1986; Wunsch 1988; Thacker 1989; Tziperman and Thacker 1989; Bennett and Thorburn 1992). The objective function is a sum of quadratic terms penalizing misfit between the observations and the data produced by the model, and also penalizing corrections to the assumed model parameters, including forcing, initial conditions, and boundary conditions. The weighting of the penalty terms may include smoothness criteria, and the forcing errors may include errors in the model equations at every point in space and time (Bennett and Thorburn 1992). A global inverse method similar to the "Green's function method" (Wunsch 1996) was used to fit the regional PE model to the hydrographic data of a CalCOFI survey covering about 3 weeks by adjusting the initial state of the model. Because the model forcing and boundary conditions were not adjusted, the model evolution depended only on the initial conditions.

The starting guess for the model's initial conditions came from a time-independent, three-dimensional objective analysis of the CalCOFI observations, treated as if they were simultaneous at the start of the survey. The model was run from this poorly resolved initialization, and the modeled data were compared to the raw observations throughout the duration of the CalCOFI survey (fig. 2).

The misfits between the model and the observation were corrected by adjusting the initial conditions based on Green's functions that relate changes in the model's initial conditions to changes in the model's estimates of the observations. The model's initial state was adjusted to minimize the sum of the squared, normalized misfits between the observations and the temperatures and salinities predicted by the model at all the data points over the time range, while also minimizing the sum of squares of the normalized changes to the model's initial conditions. The changes to the initial conditions are expanded in sinusoids in the horizontal and smooth functions (EOFs) in the vertical, so the minimization procedure

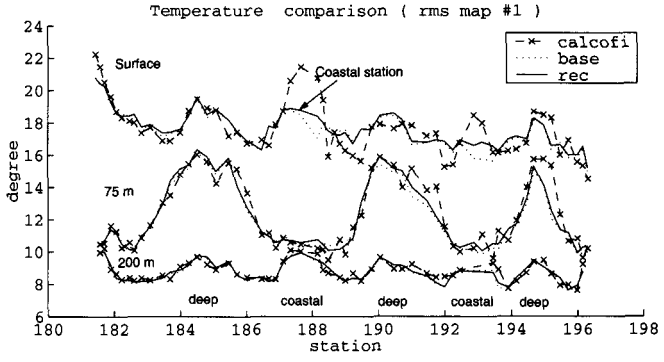

Figure 2. Observed (—x—) and modeled temperature at 0, 75, and 200 m plotted along-track as a function of station for the July 1997 CalCOFI cruise. The base model run (dotted line) is initialized from an objective analysis of the CalCOFI hydrographic data. The model run using the correction to initial conditions provided by the inverse solution (solid line) shows reduced misfit mainly in the shallow near-coastal stations.

includes smoothness constraints by penalizing short length scales more than long scales. The assimilation retains the form of objective mapping as a least-squares fit (Davis 1985), with the data covariance matrix derived from the time-dependent Green's functions and the model parameter covariance. Setting the model's covariance controls the smoothing constraints, and the data error covariance governs the fit to the data.

Errors in fitting to the data were assumed to come both from errors in the observations and from model errors due to the linearization, the limited set of initial perturbations, and the limited horizontal and vertical resolution. The assumed data error bars were checked against the final misfits ("residuals") after the fit, to assure that the assumptions had not been violated, and that no single datum exerted significant influence on the estimate. Because advection is important in this example, the linear Green's functions depend on the initial state, so the estimation procedure must be iterated. Miller and Cornuelle (1999) provide further details of our fitting procedure in the context of a different oceanographic region.

TESTS OF THE DYNAMICAL FITS

The fitting procedure was tested for the July 1997 CalCOFI survey (cruise 9707) when El Niño conditions prevailed in the tropical Pacific. At this time, the initial signal of El Niño in California waters was observed as an increase in the coastal undercurrent, which transported unusually warm waters northward at depths below 100 m (Lynn et al. 1998). Local changes in the wind forcing due to the atmospheric teleconnections with El Niño followed only in November 1997.

The general view of the physical structure from CalCOFI hydrography at this time shows the core of the California Current system (CCS) to be displaced slightly farther west than usual (Lynn et al. 1998).

A well-defined inshore countercurrent, evident in both temperature and salinity, with greater-than-average velocity was observed. A vertical section along CalCOFI line 93 shows a plug of water with salinity exceeding 34.4 at the 200 m depth level that was not found during the previous cruise. The ADCP velocities confirm a strong and continuous poleward California Undercurrent through the SCB and around Point Conception that advects highly saline and warm waters from the southern boundary. This pattern is thought to be related to the coastally trapped Kelvin-like waves excited by the strong El Niño event in the tropics.

Initialization Procedure and Forcing

In order to commence the model fitting procedure, an initial ocean state must be constructed to be as close as possible to the (unknown) observed one. Observations for the nonsynoptic three-dimensional temperature and salinity fields are available only in the small "CalCOFI subdomain," for which we use the cruise data for temperature and salinity as a time-independent picture of the ocean. Further data (Leetmaa Pacific Ocean Analysis provided by the Climate Diagnostics Center *http://www.cdc.noaa.gov/cdc/data.leetmaa.html*) are used to fill in the ocean's initial state outside this region in a smooth way.

Before merging the two data sets, we confirmed that the vertical structure of the Leetmaa data compared well with the CalCOFI data for July 97. We merged the two data sets by making an objective map over the entire model domain of the anomalous temperature and salinity fields defined as Leetmaa minus CalCOFI. Merging data sets during other cruise periods is not always practicable in this way, and further treatment of the data is required. For example, for the February 1998 cruise the vertical analysis revealed some discrepancy in the profiles at depth in both temperature and salinity around the perimeter of the CalCOFI subdomain. This is due to the smoothing implicit in the Leetmaa data, which is an assimilation of data with an ocean model. The salinity data used in the assimilation are inadequate to properly resolve the vertical structure in the proximity of the coast. The horizontal gradients in density produced by these discrepancies generate strong adjustment currents at depth, which are artificially induced by the matching. We therefore computed a mean vertical profile anomaly for temperature and salinity in the CalCOFI subdomain and subtracted this anomaly from all Leetmaa data. We then defined a horizontal anomaly as CalCOFI data minus Leetmaa at each depth. Before objectively mapping the anomalies on the entire model grid, we also fit a smooth plane to account for horizontal large-scale background gradients in temperature and salinity. This initial guess will subsequently be corrected by the inverse solution.

The initial velocity field for the model is also critical in that it should be nearly geostrophically balanced with the horizontal density gradients. We initially computed geostrophic currents from the density fields. We assumed a level of no motion at around 1,000 m, since we know that the core of the CCS can easily extend down to 500 m with velocities on the order of 0.2 cm/sec (Chereskin and Trunnell 1996). The problem with this calculation is that the initial kinetic energy state of the model is not in equilibrium, and integration over time shows a sharp spin-up of the velocity field during the first day. In order to compute sensitivity to initial conditions with the inverse method, it is not useful to allow this spin-up process. Therefore we have computed the initial velocity field by integrating the model forward in time for half a day, keeping the density constant and with no forcing. This second approach insures a more balanced energetic state in the initial condition. We eventually will correct this first-guess initial velocity state by using the inverse method.

For the forcing fields we use Levitus climatology for heat fluxes and COADS monthly wind stress. The time span of the cruise is about three weeks. In later experiments we plan to investigate the sensitivity to higher frequency in the forcing and how this affects our fitting and forecasting time scales.

Basis Functions for Assessing Sensitivity

As described in the section "Inverse Method Fitting Technique," we project the error field between model and observed initial conditions onto a reduced space. The optimal basis to be chosen for this projection is not known, so we arbitrarily picked the Fourier basis sets of sines and cosines for horizontal structures as a first try. In the vertical, we used empirical orthogonal functions (EOFs) of the difference between CalCOFI observations and model-derived temperature and salinity profiles from the base run from first-guess initial conditions. These vertical modes tend to show maximum variability at roughly 100 m, with about 70% of the variance explained by the first EOF and 20% by the second.

Initial tests of the model runs' sensitivity to slight changes in the initial conditions when we used these basis functions showed strong nonlinearity in the upper ocean. That is, a large-scale, small-amplitude perturbation in temperature or salinity resulted in a time-dependent perturbation from the base run that had large amplitudes at the grid scale after only a few days. We traced this nonlinearity to the model KPP mixed-layer parameterization (Large et al. 1994), which gives a time- and space-dependent vertical diffusion coefficient based on a number of criteria. Since this strong nonlinearity would complicate the linear fitting procedure, we set the vertical diffusion to be a constant chosen to yield

reasonable mean and eddy variance states. When surface-forced mixed-layer processes are addressed in future work, we plan to reexamine the KPP framework in the context of the linear inverse.

Results of the Inverse

We ran a total of 500 perturbation runs for temperature and salinity, resolving up to six wavenumbers in each horizontal direction and three vertical modes. Each model run is sampled in time as the CalCOFI cruise sampled the real ocean. Each perturbation run is the model's forecast for the cruise from a slightly different initial state.

In the application of the inverse, we also need to assign rms fitting error to each datum. The error includes both observational error and representational error, which comes from the inability of the model to reproduce all the physical processes seen in the data (e.g., internal waves). Our first fitting attempt used a constant rms-error-bound for each observation. However, the results (fig. 2) tended to place more emphasis on fitting the coastal station data where the mismatch is highest. Since we anticipate that slow open-ocean eddies will be better resolved by model physics than fast shallow-water coastal eddies, we next attempted to allow a larger fitting error in the coastal region than offshore.

In order to better minimize the misfit in the deep ocean, we redefined an rms-error-bound map based on the spatial distribution of the station, with larger error for coastal than offshore stations. Since the inverse is a linear method, we also took into account the level of nonlinearity of each individual station in the rms-error-bound map. A test of the nonlinearity can be obtained by rerunning many of the perturbation runs with the opposite sign of the perturbation amplitude. The difference in the response to the positive and negative perturbations is an estimate of the nonlinearity in the response. If we map this variance horizontally we see that nonlinearities are stronger in the coastal region, as we would expect. An error variance reduction of 68% was obtained with this new rms-error-bound map definition, and a better fit of the offshore eddies was achieved, as can be seen in figure 3.

Figure 4 shows the time-dependent map of 50 m temperature from the model run from the corrected initial state for the CalCOFI cruise in July 1997. The slow evolution of the larger mesoscale eddies offshore and the more rapid evolution of the smaller eddies nearshore suggests that we have a much better chance of skillfully fitting the offshore thermocline eddies than the near-coastal squirts and jets with the available data. More highly resolved observations in space and time will be needed for near-coastal fits. Likewise, processes in the surface mixed layer are not skillfully modeled here because time-dependent surface forcing is not included and because of the limited oceanographic data.

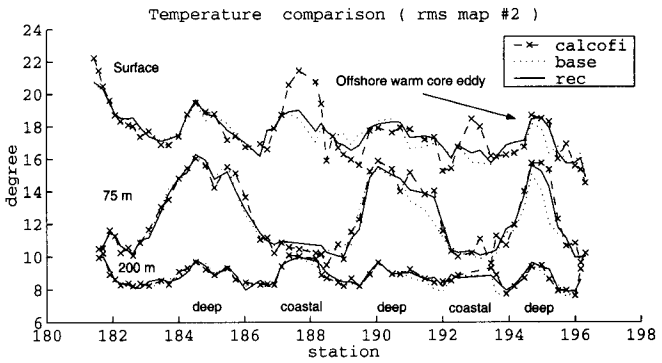

Figure 3. Same as figure 2 but for inverse solution using observational rms-error-bounds that are larger for near-coastal data than for deep-ocean data.

TESTS OF THE BIOLOGICAL MODEL

The biological fields are strongly influenced by the physical variations. Therefore, once a physics fit is complete, it can be used to drive the biological model as a first test. The first SeaWiFS images were collected in September 1997, so our tests of the July 1997 physical field fits are not suitable for testing the ecosystem model. The best-sampled CalCOFI period after SeaWiFS began is February 1998 (cruise 9802), so we began testing the 4D biological model for that period. We first want to understand how sensitive the biological model is to the various terms that influence it.

We created an initial chl a field for the CalCOFI domain from daily 9 km SeaWiFS imagery collected during the cruise 9802 period. A 5-day running average was applied to the resulting 19-day, 2D chl a time series to insure minimal pixel dropout. Remaining holes in the images were removed by iteratively averaging from the hole edges into the hole centers. Finally, the 2D time series was interpolated to the ROMS West Coast model grid. For the purpose of initializing the 3D chl a field, we selected the first 2D field in the averaged time series, corresponding to the 5-day average centered around day 3 of the 9802 cruise, and calculated the subsurface chl a distribution. Following Morel and Berthon (1989), this calculation produces a Gaussian distribution of chl a between the surface and the light penetration depth as defined by the SeaWiFS chl a concentration (fig. 5a). We set the chl a concentration to zero for all depths greater than the penetration depth. Vertical integration of the 3D model field reproduces the horizontal distribution as seen by SeaWiFS (fig. 5b). The 3D chl a field was added to the physical model as a passive tracer, and 30-day model runs were made with and without diffusion.

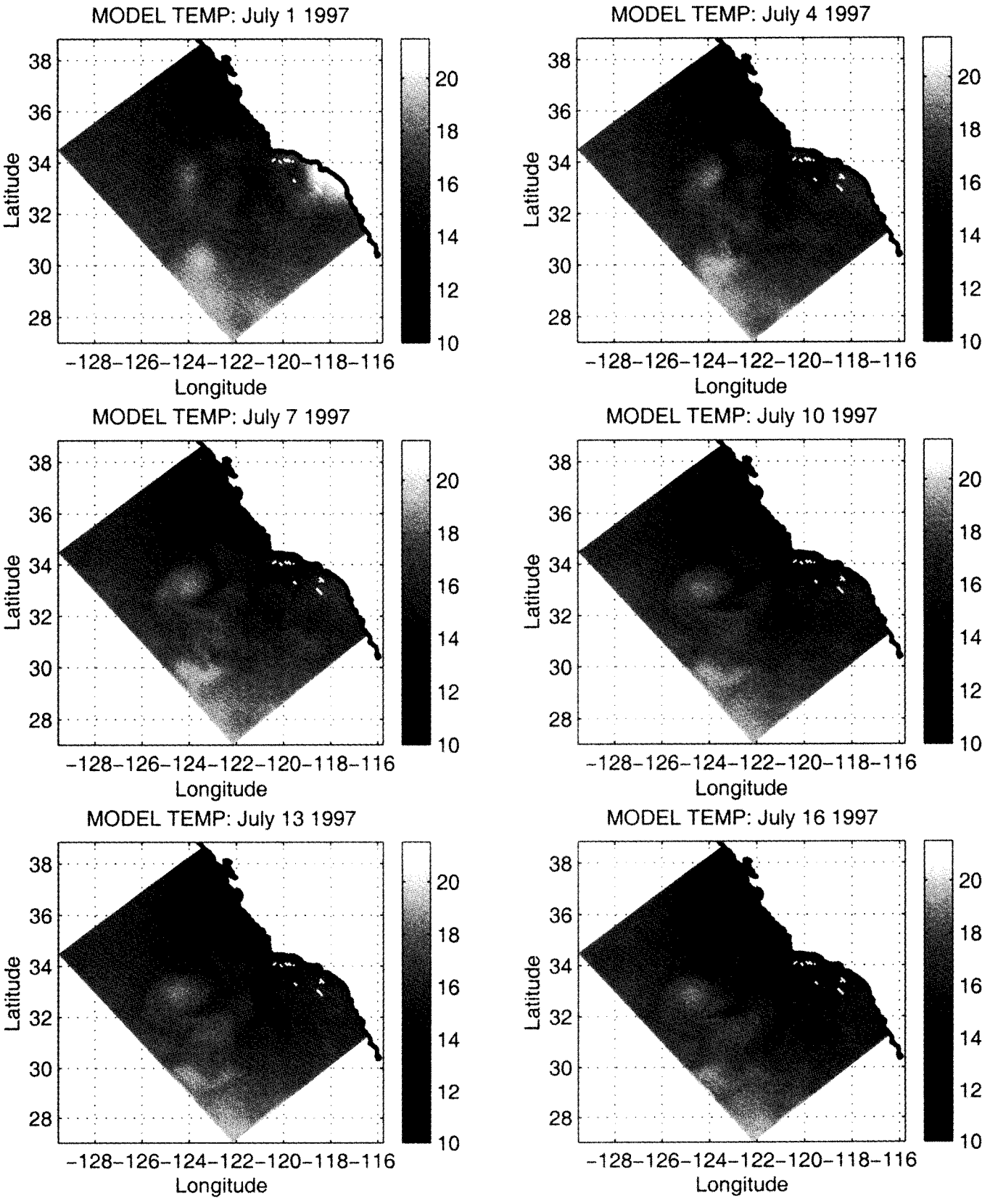

Figure 4. Time sequence of model temperature at 50 m depth from the case where the model's initial conditions have been corrected by the inverse method with rms-error-bounds larger in the near-coastal region.

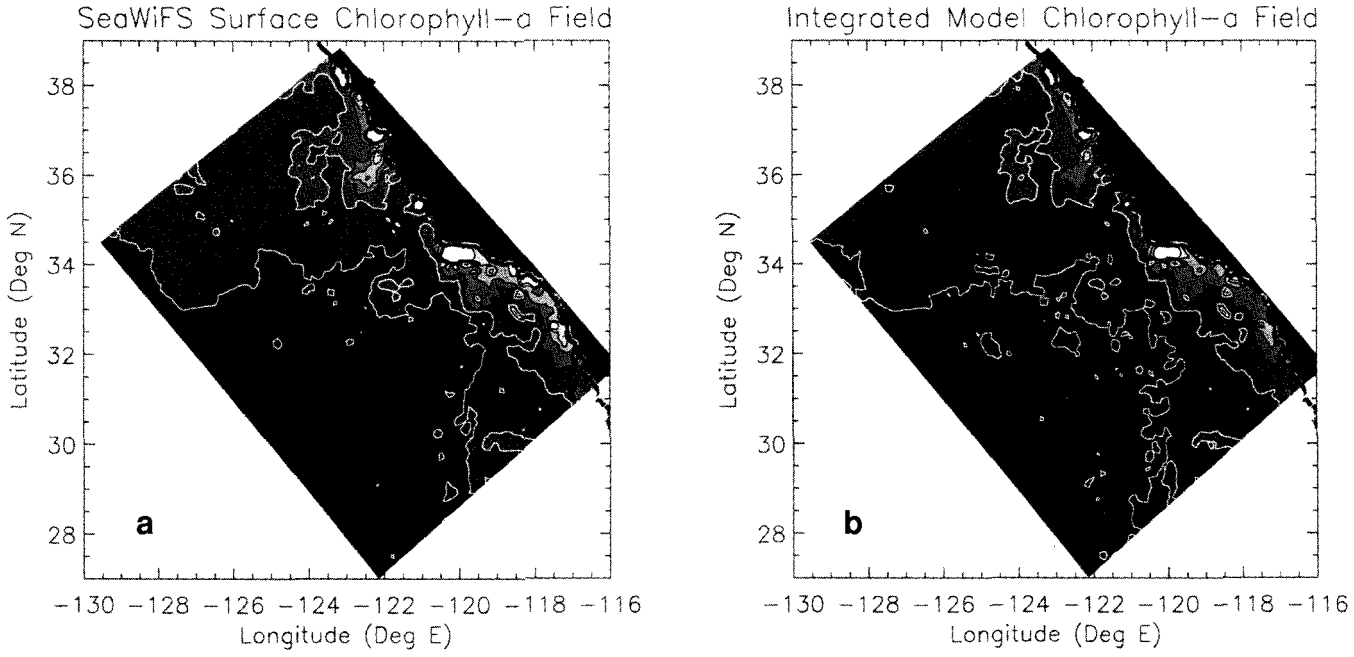

Figure 5. Comparison between *a*, raw 5-day average SeaWiFS image of chl a (integrated from the surface to one optical depth) and *b*, SeaWiFS-derived model initial condition of chl a (integrated from surface to ocean bottom) for the beginning of 9802 CalCOFI survey. SeaWiFS image contours range from 0.01 in the open ocean to peak values near 0.4 in the shallow-water regions. Model image contours are proportional to SeaWiFS by an unspecified factor.

3D Ecosystem Model Evolution

Examination of the SeaWiFS record for the 9802 period reveals a persistent chl a signature in the coastal waters. In animations of both the SeaWiFS imagery and model output, this coastal chl a is generally moved north or south along the coast with agreement between the two data sets as to direction. As would be expected, without replacement of the chl a via production, the modeled chl a tracer is quickly lost from the coastal waters and transported either offshore or to deeper depths. The pattern of movement is different depending on whether vertical or horizontal diffusion is present in the physics, but the end result, without active biological production, is still a general loss of chl a from the coastal surface waters.

We are now investigating how various pathways in the 7-component model affect the spatial distribution of chl a in the model. Starting at the simplest: chl a and phytoplankton with uptake of nitrate and parameterized loss, we intend to add components and pathways incrementally until we have the full 7-component model running over the CalCOFI domain. Although the full model has already been run successfully, this approach will allow us to examine the biological response of the model while comparing the results to both the CalCOFI 9802 data set and associated SeaWiFS imagery. The incremental approach will also allow us to rigorously determine many of the rate and flux parameters associated with the model.

1D Ecosystem Model Performance

Because many of the parameters in the ecosystem model are poorly known, we have investigated the model's sensitivity over a wide range of parameters. Our approach has been to use a one-dimensional mixed-layer model that has been coupled to the ecosystem model. We have tested this model at two extrema in the CalCOFI domain, the coastal and the offshore regions. The model is initialized with climatological profiles of temperature, salinity, and nitrate that were obtained from each of the two regions. The climatological profiles are also used as nudging fields for the temperature, salinity, and nitrate profiles. The nudging time scale is set to a constant 5 years. All other model variables are set to a constant value and are not nudged. In order to further diagnose the model's results, we added an oxygen component to the model to track the effects of the remineralization process. The oxygen value is set to the saturation value at the surface for the given SST. The simulations are carried out for 10 years, which is enough time to allow the model to develop a steady seasonal cycle.

By reducing the ecosystem model testing to a 1D problem, we are able to examine many cases by using different parameter sets. The model's results are compared against the climatological profiles of temperature, density, nitrate, chl a, and oxygen that were obtained from the CalCOFI data set. An example of one such comparison (fig. 6) demonstrates that the model is capable of resolving several of the observed features. The

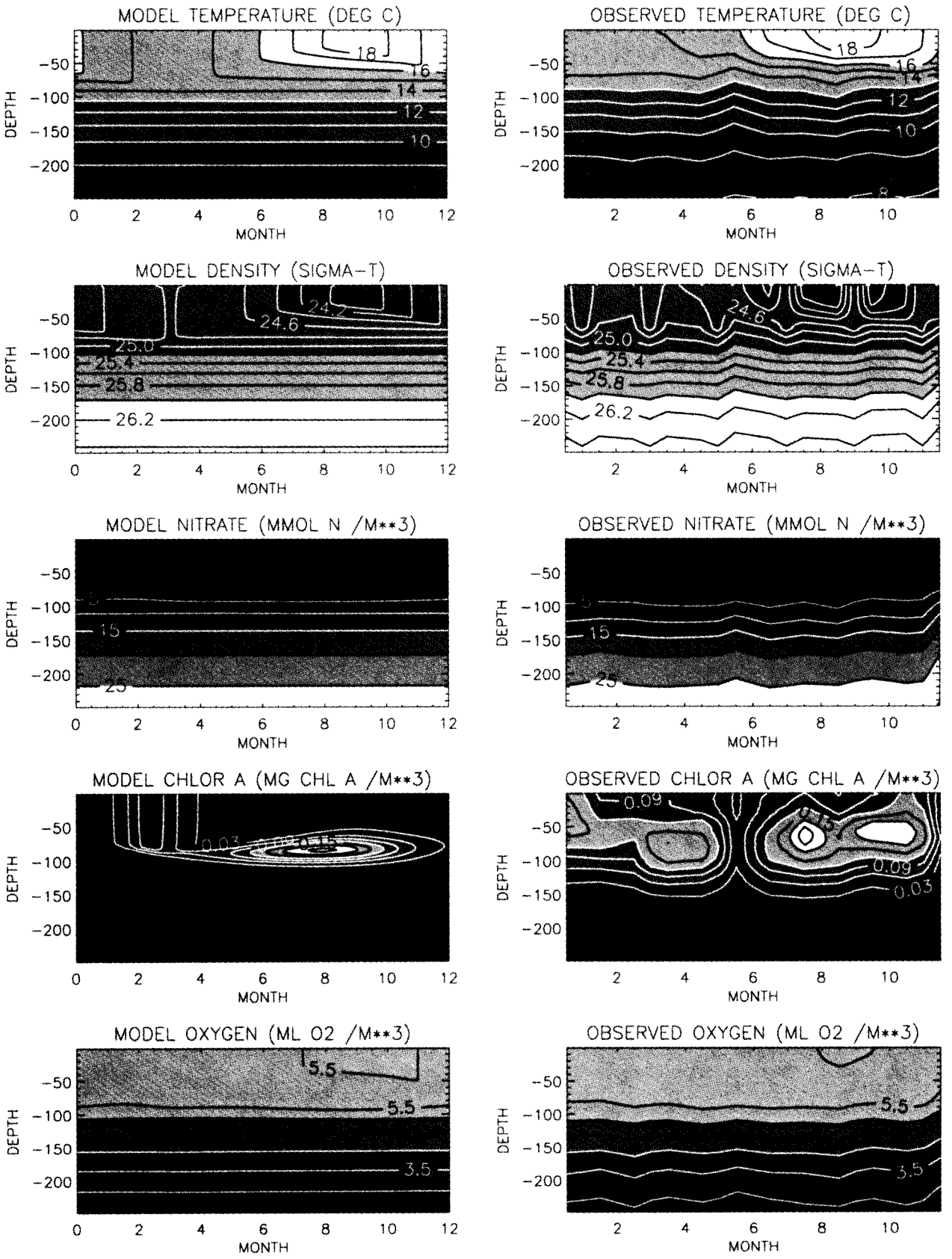

Figure 6. Comparison between 1950–99 mean seasonal cycle CalCOFI offshore profiles (*right*) and 1D mixed-layer/ecosystem model simulation with seasonal cycle climatological forcing (*left*). Plotted are (*top to bottom*) temperature, density, nitrate, chl a, and oxygen profiles from 0 to 250 m and from January to December.

mixed-layer model is capable of resolving the seasonally varying SST and mixed-layer depths. The nitracline is well established at about 100–150 m, with very low concentrations at the surface. Surface chl a is highest in the winter, with an established chl a maximum at about 80–90 m. Unfortunately, the chl a climatologies had to be averaged over 2 months in order to achieve a smoothly varying chl a field. One issue that has yet to be resolved is why the model creates such a thin chl a maximum at depth while the data suggest a wider feature. Part of this discrepancy may be due to the averaging of many profiles to obtain the climatologies of the data set. The oxygen profile from the model compares well with the climatologies and shows a gradual decline in oxygen levels with depth and a sub-mixed-layer oxygen maximum during the summer.

We are now configuring the 1D model to the coastal CalCOFI climatologies. After we have achieved good agreement between both offshore and coastal locations, we will compare the resulting parameter sets to try to resolve the differences between regions. The parameter sets which result from the 1D simulations will be used as a starting point for the full 3D data assimilation of both the circulation and ecosystem models.

SUMMARY AND OUTLOOK

Our initial test of the fitting procedure successfully reduced the error variance of the model-data misfit in temperature and salinity by nearly 70% during the July 1997 CalCOFI cruise. These encouraging results suggest that we should eventually be able to reduce the misfits even further by including adjustments to horizontal velocity and sea level. We are presently preparing the TOPEX, ADCP, and drifter data to additionally constrain the fit.

Our success so far is geared toward deep-ocean thermocline eddies, which evolve slowly and geostrophically. Progress in fitting the shelf-slope eddies will be hindered by limitations in the volume of data needed to constrain these faster and smaller-scale features. Progress in fitting the upper-ocean mixed-layer variations will depend on the quality of surface-forcing data from atmospheric analyses or direct observations, because these oceanic features are strongly influenced by direct atmospheric forcing rather than by intrinsic oceanic instabilities.

Fits of the ecosystem variations are likewise limited by the small amount of subsurface data available and the great uncertainties in coupling parameters between the biological variables. Nonetheless, since the physical variations control the biological variations to a large degree, we expect to successfully match the available data to within error bars.

Once the fits are complete for a given survey, we will break down the dynamical and ecosystem balances that hold in the model and assess their consistency with other modeling studies. The true test for the model and the inverse technique is to forecast independent data in subsequent CalCOFI hydrographic and ADCP surveys, TOPEX data sets, and SeaWiFS observations. Since there was monthly sampling (albeit limited spatial sampling) during the 1997–98 El Niño, we expect to be able eventually to quantify predictive time scales for this region.

ACKNOWLEDGMENTS

We gratefully acknowledge funding from NASA (NAG5-6497) and ONR (N00014-99-1-0045). Supercomputing resources were additionally provided by the San Diego Supercomputer Center. We thank our colleagues at Rutgers University (Hernan Arango, Kate Hedstrom, and Dale Haidvogel) and UCLA (Sasha Shchepetkin, Patrick Marchesiello, and Jim McWilliams) for generously allowing use of their computer models and for aiding in many aspects of this work. We also thank our CalCOFI colleagues (Teri Chereskin, Peter Niiler, Ron Lynn, and Tom Hayward) for providing data in accessible form and for many important discussions.

LITERATURE CITED

Bennett, A. F. 1992. Inverse methods in physical oceanography, monographs on mechanics and applied mathematics. New York: Cambridge University Press, 346 pp.

Bennett, A. F., and M. A. Thorburn. 1992. The generalized inverse of a nonlinear quasi-geostrophic ocean circulation model. J. Phys. Oceanogr. 22:213–230.

Bograd, S. J., T. K. Chereskin, and D. Roemmich. In press. Transport of mass, heat, salt and nutrients in the California Current system: annual cycle and interannual variability. J. Geophys. Res.

Chereskin, T. K., and M. Trunnell. 1996. Correlation scales, objective mapping, and absolute geostrophic flow in the California Current. J. Geophys. Res. 101:22,619–22,629.

Davis, R. E. 1985. Objective mapping by least squares fitting. J. Geophys. Res. 90:4773–4778.

Fasham, M. J. R., H. W. Ducklow, and S. M. McKelvie. 1990. A nitrogen-based model of plankton dynamics in the oceanic mixed layer. J. Mar. Res. 48:591–639.

Ghil, M., and P. Malanotte-Rizzoli. 1991. Data assimilation in meteorology and oceanography. Adv. Geophys. 33:141–266.

Hayward, T. L., and E. L. Venrick. 1998. Nearsurface pattern in the California Current: coupling between physical and biological structure. Deep-Sea Res. II 45:1617–1638.

Large, W. G., J. C. McWilliams, and S. C. Doney. 1994. Oceanic vertical mixing—a review and a model with a nonlocal boundary-layer parameterization. Rev. Geophys. 32:363–403.

Le Dimet, F.-X., and O. Talagrand. 1986. Variational methods for analysis and assimilation in meteorological observations. Tellus 38:97–110.

Lynn, R. J., T. Baumgartner, J. Garcia, C. A. Collins, T. L. Hayward, K. D. Hyrenbach, A. W. Mantyla, T. Murphree, A. Shankle, F. B. Schwing, K. M. Sakuma, and M. J. Tegner. 1998. The state of the California Current, 1997–1998: transition to El Niño conditions. Calif. Coop. Oceanic Fish. Invest. Rep. 38:25–49.

Miller, A. J., and B. D. Cornuelle. 1999. Forecasts from fits of frontal fluctuations. Dyn. Atmos. Oceans 29:305–333.

Moisan, J. R., E. E. Hofmann, and D. B. Haidvogel. 1996. Modeling nutrient and plankton processes in the California coastal transition zone 2. A three-dimensional physical-bio-optical model. J. Geophys. Res. 101:22,677-22,691.

Morel, A., and J.-F. Berthon. 1989. Surface pigments, algal biomass profiles, and potential production of the euphotic layer: relationships reinvestigated in view of remote-sensing applications. Limnol. Oceanogr. 34:1545–1562.

Roemmich, D., and J. McGowan. 1995. Climatic warming and the decline of zooplankton in the California Current. Science 267:1324–1326.

Song, Y. H., and D. Haidvogel. 1994. A semi-implicit ocean circulation model using a generalized topography-following coordinate system. J. Comput. Phys. 115:228–244.

Thacker, W. C. 1989. The role of the Hessian matrix in fitting models to measurements. J. Geophys. Res. 94:6177–6196.

Tziperman, E., and W. C. Thacker. 1989. An optimal-control adjoint-equations approach to studying the oceanic general circulation. J. Phys. Oceanogr. 10:1471–1485.

Wunsch, C. 1988. Transient tracers as a problem in control theory. J. Geophys. Res. 93:8099–8110.

———. 1996. The ocean circulation inverse problem. Cambridge Univ. Press. 442 pp.